JOURNAL OF MATERIALS SCIENCE **36** (2001) 3809–3815

Effects of particle size of $BaTiO_3$ powder on the dielectric properties of $BaTiO_3$/polyvinylidene fluoride composites

HSING-I HSIANG
Department of Materials Science and Engineering, I-Shou University, Kaoshiung, Taiwan, 84008, Republic of China
E-mail: hsingi@mail.ttn.com.tw

KWO-YIN LIN, FU-SU YEN, CHI-YUEN HWANG
Department of Mineral and Petroleum Engineering, National Cheng Kung University, Tainan, Taiwan 70101, Republic of China

The effects of particle size of fine $BaTiO_3$ powder on dielectric properties of $BaTiO_3$/polyvinylidene fluoride (PVDF) composites were investigated. When the frequency of the applied field was less than 100 kHz, the dielectric constant and loss for $BaTiO_3$/PVDF composites decreased with increasing $BaTiO_3$ particle size. When the frequency was greater than 100 kHz, the opposite results were obtained. The resistivity increased with increasing $BaTiO_3$ particle size, whereas the open areas of hysteresis loops decreased gradually. The degree of poling efficiency for $BaTiO_3$/PVDF composites increased with increasing $BaTiO_3$ particle size. The $BaTiO_3$ particle size dependence of the dielectric properties of $BaTiO_3$/PVDF composites is explained by space charge effects at the interface between $BaTiO_3$ and PVDF, and domain configurations (single or multi-domain) of the $BaTiO_3$ powders. © *2001 Kluwer Academic Publishers*

1. Introduction

Much research has been done on ceramic/polymer composites, especially for piezoelectric application of an electromechanical transducer. Many connectivity patterns are designed for use in hydrophone, sonar, and biomedical applications [1–3]. Among the composites, the simplest type is the 0–3 connectivity, which consists of a three-dimensionally connected polymer matrix loaded with piezoelectrically active ceramic particles [4]. An attractive feature of the 0–3 design is its versatility in fabricating various forms including thin sheets, and certain molded shapes. A composite of this type is also easily fabricated and amenable to mass production.

The dielectric properties of $BaTiO_3$ depend strongly on the size of the crystallites [5] and the domain configuration [6]. Surface and size effects on ferroelectric phase transitions have been investigated [7, 8]. The dynamics of domain wall movement were examined for ceramics and single-domain crystals [9]. The relationship between AC field and polarization (hysteresis loop) of $BaTiO_3$ is affected by the tetragonal-to-orthorhombic phase transition [10] and the domain configuration (single domain or multi-domain) [9]. The dielectric constant of powdered $BaTiO_3$ (>2 μm) was small but increased with increasing particle size [11, 12]. Goswami [12] attributed the small dielectric constant to a surface defect layer with a low dielectric constant existing on the particle surface, because the smaller the particle size, then the greater the surface layer effect. Newnham *et al.* [13] expected variation of dielectric properties with decreasing size of $BaTiO_3$ particles to follow the magnetic analogue closely. For small particles, as the size decreased, a single domain might be formed within the crystallite, and the dependence of dielectric constant on the crystallite size differed significantly from that of multi-domain samples. Research on the size dependence of the phase transition, domain configuration and dielectric properties of ultrafine $BaTiO_3$ (<1 μm) powders is not reported.

For $BaTiO_3$/polyvinylidene fluoride (PVDF) composites, dielectric, hysteresis and pyroelectric behaviour was previous evaluated [14–17]. The domain configuration and the phase transition of $BaTiO_3$ powder can affect the dielectric properties of $BaTiO_3$/PVDF composites [14, 15]. Furthermore the domain configuration and phase transition of $BaTiO_3$ powder are controlled by the crystallite size, although the effect of particle size on dielectric properties of $BaTiO_3$/PVDF composites is poorly understood. The purpose of our work was to investigate the dependence on particle size of dielectric properties of $BaTiO_3$/PVDF composites of 0–3 type.

0022–2461 © *2001 Kluwer Academic Publishers*

2. Experimental procedure

2.1. Sample preparation

Samples of $BaTiO_3$/PVDF composites of 0–3 type were prepared according to methods reported by Sekar *et al.* [15] $BaTiO_3$ powder was prepared by calcining barium titanyl oxalate tetrahydrate (Central Glass Co., Ltd, Japan) at 700–1300°C for 2 h to obtain $BaTiO_3$ particles of varied particle size. To prepare the samples, the calcined $BaTiO_3$ powder was mixed with PVDF in a ratio of 40 vol% (70 wt%) as it shows good connectivity between $BaTiO_3$ and PVDF [16, 17], with acetone as thinner so that all grains of $BaTiO_3$ were wholly wetted with polymer after the mixture dried. The composite powders were then hot pressed at 180°C for 10 min under a pressure of 130 MPa, in a steel die of diameter 12 mm. The die was cooled to room temperature under the applied pressure.

2.2. Characterization

An X-ray diffractometer (XRD)(Rigaku) was used to identify the $BaTiO_3$ phases of the calcined powders and the surfaces of the composites. The lattice parameters of $BaTiO_3$ powders were determined by using (111), (200), and (002) peaks. Ferroelectric domain width was determined using the Scherrer equation [18]. The (222) peak was used to calculate crystallite size, because no interference occurs from other diffraction peaks. The Feret diameter [19] of as-calcined $BaTiO_3$ powders was performed using transmission electron microscopy (TEM)(200CX, Jeol, Tokyo, Japan) micrographs. Specific Surface areas were measured using the conventional nitrogen absorption (BET) technique (Gemini 2360, Micromeritics) and equivalent spherical diameters were calculated from the surface areas. Air dried conducting silver paste (D-550, Dotite, Japan) was applied to the surface of pellets by screen printing. The dielectric constant and dissipation factor of the pellets were measured at frequencies from 100 Hz to 10 MHz. The resistivity of $BaTiO_3$/PVDF composites was measured by high resistance meter (HP 4329A). The hysteresis loops were measured with a modified Sawyer-Tower circuit. A sinusoidal field of 10 kV/cm and 60 Hz was applied to the sample during measurements. The $BaTiO_3$/PVDF composites were poled with a field of 1 MV/m and 30 MV/m for 15 min in a silicon oil bath. After poling, the degree of poling efficiency could be identified by the reversal of X-ray intensity in (200) and (002) peaks, i.e., $I_{(002)} < I_{(200)}$ before poling and $I_{(002)} > I_{(200)}$ after poling.

3. Results and discussion

3.1. Particle size measurement

Thin twins in crystal lattices are well known to cause a general broadening effect of Bragg reflections [20]. Measurements of these broadenings can be used to measure the width of the twins in the $BaTiO_3$ powders. Therefore, the domain size determined in a t-$BaTiO_3$ crystallite using the Scherrer equation should be equivalent to its ferroelectric domain [21]. Fig. 1 shows the particle sizes of samples measured using XRD, TEM and BET techniques. The XRD measurement determines the ferroelectric domain size in the crystals. TEM provides an image of particles which may be single crystals or crystal aggregates. The BET measurement determines the aggregate size. Each t-$BaTiO_3$ crystallite consists of one (single-) or more (multi-) ferroelectric domain. Thus, the size measured using TEM is larger than that using XRD. Both the ferroelectric domain and crystallite size of the as-calcined powders became larger with increasing calcination temperature (Fig. 1). At 700–1000°C, the size measured using XRD is close to that using TEM. Obviously, the crystallites are single domain c- or t-$BaTiO_3$. The size deviation between the XRD and TEM measurements became larger as the temperature increased above 1000°C due to the occurrence of aggregation and domains. Therefore the size measured using TEM is close to that using BET. Unless specified, the particle sizes reported in the following results were all measured by TEM technique.

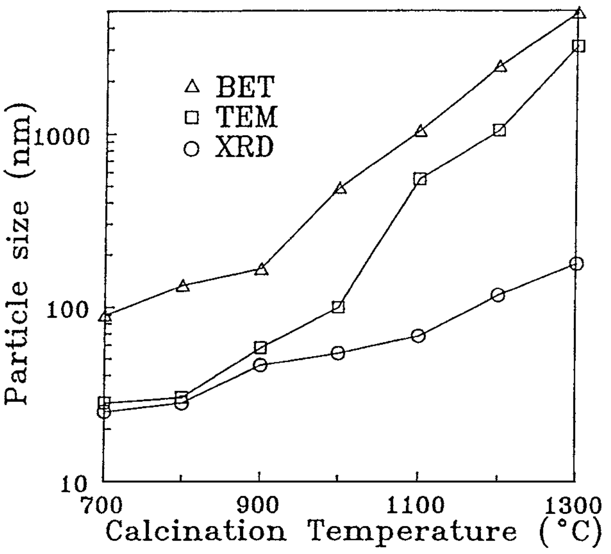

Figure 1 Particle sizes of $BaTiO_3$ powders calculated by XRD, TEM and BET techniques for different calcination temperature.

3.2. X-ray diffraction

Fig. 2 shows the diffraction patterns of $BaTiO_3$ powders calcined at varied calcination temperature. There is little change in the X-ray diffraction patterns for the composites compared to the powder. The intensity of the peaks of PVDF have not been seen at all in the composites, as reported by Muralidhar *et al.* [4]. The barium titanate powders calcined at 700 and 800°C were cubic [22]. With increasing calcination temperature the (220) split into (202), (220) reflections of t-$BaTiO_3$. According to Fig. 2, no tetragonal line splitting of the X-ray reflection was detected on smaller $BaTiO_3$ particles calcined at a temperature below 900°C. Compared with the X-ray reflections of calcined powders, only a line shift to smaller reflection angles and a line broadening were observed in the composites. Fig. 3 shows variations of the lattice parameter for $BaTiO_3$ powders. The lattice parameter of $BaTiO_3$ powders decreased with increased particle size measured by TEM technique.

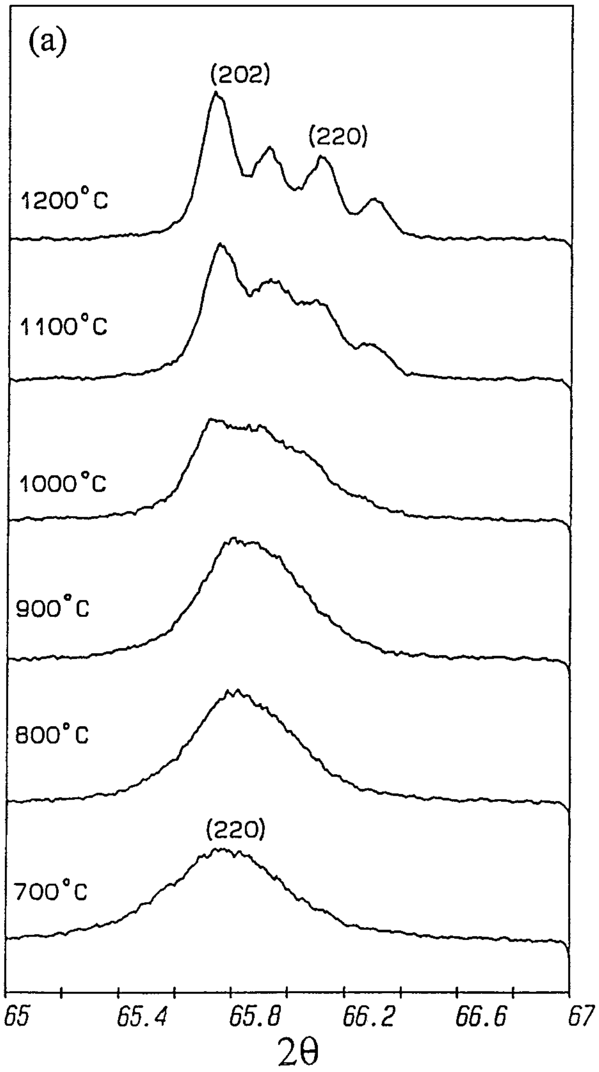

Figure 2 XRD patterns of the $BaTiO_3$ powders calcined at different calcination temperatures.

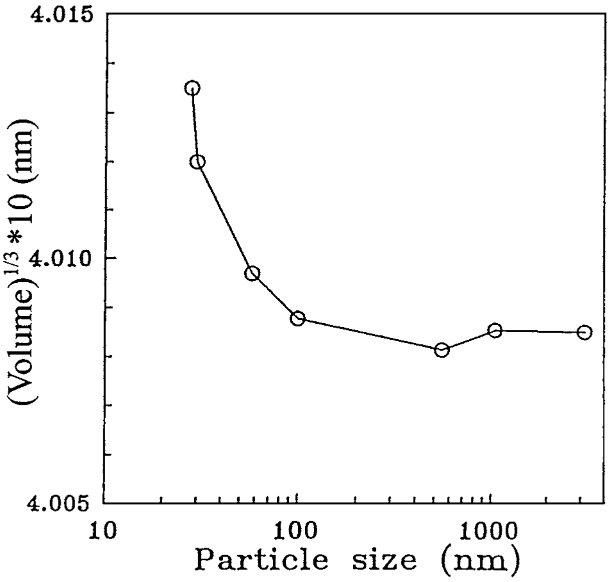

Figure 3 Variations of lattice parameter of as-calcined powders as a function of $BaTiO_3$ particle size.

3.3. Morphology

Fig. 4 shows the morphologies of $BaTiO_3$ particles calcined at 700–1200°C. In this figure, fine sub-rounded particles with narrow particle-size distribution and limited aggregation are observed for the powders calcined at 700–1000°C. At higher calcination temperatures, increased crystallite size and hard agglomeration were observed. In $BaTiO_3$-PVDF composites, they appear homogeneous and the two phases are randomly interconnected. Similar results were observed by Muralidhar *et al.* [17].

3.4. Dielectric constant measurements and dissipation factor

The variations of dielectric constant and dissipation factor with frequency for $BaTiO_3$/PVDF composites of varied size of $BaTiO_3$ particles are shown in Figs 5 and 6. The dielectric constants of $BaTiO_3$/PVDF composites at frequencies below 1 kHz increased greatly with frequency when the $BaTiO_3$ particle were smaller than 58 nm. As the particle became larger than 58 nm, the variation of dielectric constant with frequency became smooth for composites with the same size of $BaTiO_3$ particle. The frequency dependency of the dielectric loss was similar to that of the dielectric constant.

The larger lattice parameter (Fig. 3) of $BaTiO_3$ powders with particle size smaller than 58 nm may be due to imperfections in the lattice due to cation and anion sites being randomly vacant. Fig. 7 shows that there is a sudden decrease of resistivity when the size of the $BaTiO_3$ particles is less than 58 nm for the composites, possibly as a result of numerous defects in $BaTiO_3$ powders of such a particle size. Under these conditions, application of a field across the interfaces of $BaTiO_3$ powders and PVDF in the composites causes more charge to be delivered to PVDF than is removed from $BaTiO_3$ powders. The resulting charge imbalance appears as a space charge at the interface. The space charge layers at the interface result in increased bound charge in phase with applied electric field. Therefore, it can be modeled with many small capacitors in series and produces an enhanced relative permittivity at low frequency in the composites.

Figs 5 and 6 demonstrate the variation of dielectric constant and dielectric loss in the $BaTiO_3$/PVDF composites with frequency and $BaTiO_3$ particle size. As the size decreases, the effects of space charges on the dielectric properties become dominant due to the increased defects in $BaTiO_3$ powders. Dielectric dispersion due to a space charge is observed at frequencies below 1 kHz. Therefore, the dielectric constant at frequency <1 kHz resulting from a space charge in $BaTiO_3$/PVDF composites of particle size less than 58 nm can be several orders of magnitude larger than the value observed at high frequency. The increase in dielectric constant and dielectric loss with decreasing frequency due to space charge effect was also reported by Muralidhar *et al.* [23]. As the frequency increased to 100 kHz, the polarization was mainly contributed from ferroelectric domains. The dielectric constants of $BaTiO_3$/PVDF composites with $BaTiO_3$ particles less

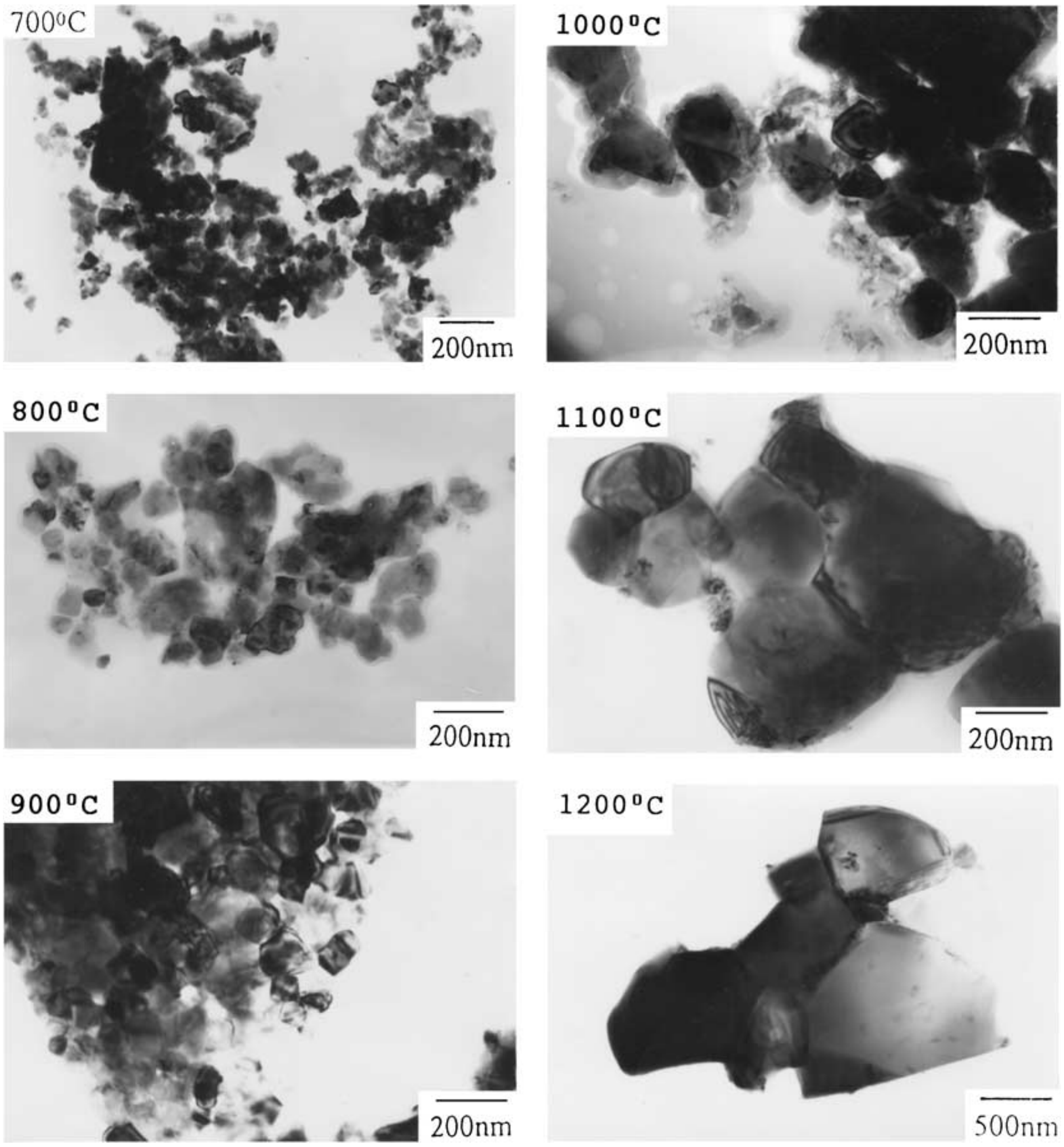

Figure 4 Transmission electron micrographs of calcined $BaTiO_3$ powders.

than 30 nm at frequencies above 100 kHz were smaller, because the crystallite phase was paraelectric cubic. Once the c-$BaTiO_3$ crystallites (powder particles) grow larger than 30 nm, the barium titanate transforms to the tetragonal phase (t-$BaTiO_3$) during cooling. A crystallite in a ceramic is clamped by its neighboring crystallites in all three dimensions during the c→t-$BaTiO_3$ phase transformation. In order to relieve the strain of transformation, ferroelectric domains form. Therefore the dielectric constants which were measured above 100 kHz for $BaTiO_3$/PVDF composites increased with increased $BaTiO_3$ particle size, because of the contribution of these domains. However, when the $BaTiO_3$ particles were larger than 550 nm, the dielectric constants of the composites declined abruptly. Perhaps a coalescence occurring at calcination temperatures above 1200°C caused particles in the powder as calcined to become a single crystal or polycrystal, so to experience a varied clamping condition. Those particles composed of one crystallite may deform like a lattice cell, being free of clamping force, and avoid forming twins from a mechanical perspective. Arlt [24] reported that the increased permittivity is possibly caused by a summation of the domain size and the internal stress effect. A greater internal stress near the grain boundary and more domain walls present in a grain may ultimately be the reason for the large K value of the $BaTiO_3$ ceramics. The removal of grain boundaries, elimination of constrained forces from neighboring crystallites and a subsequently decreased domain density as a consequence of coalescence for calcination temperatures above 1200°C and particles greater than 550 nm may induce the dielectric constant of the composites to decrease.

3.5. Poling behavior

The intensity ratio of the $I_{(002)}/(I_{(200)} + I_{(002)})$ XRD peaks from the surface of the $BaTiO_3$/PVDF composites was monitored both before and after poling to detect possible contribution of domain reorientation or rotation of single-domain or multi-domain crystallites

TABLE I The intensity ratio of the $I_{(002)}/(I_{(200)}+I_{(002)})$ XRD peaks in composites with powders calcined at different temperatures for poling fields of 0 to 3 MV/m

$I_{(002)}/(I_{(200)}+I_{(002)})$ Calcination temperature poling field	700°C	800°C	900°C	1000°C	1100°C	1200°C
0 MV/m	0	0	—	0.27	0.26	0.25
1 MV/m	0	0	—	0.27	0.33	0.37
3 MV/m	0	0	—	0.29	0.37	0.42

- It can not be divided into (002) and (200) reflection.

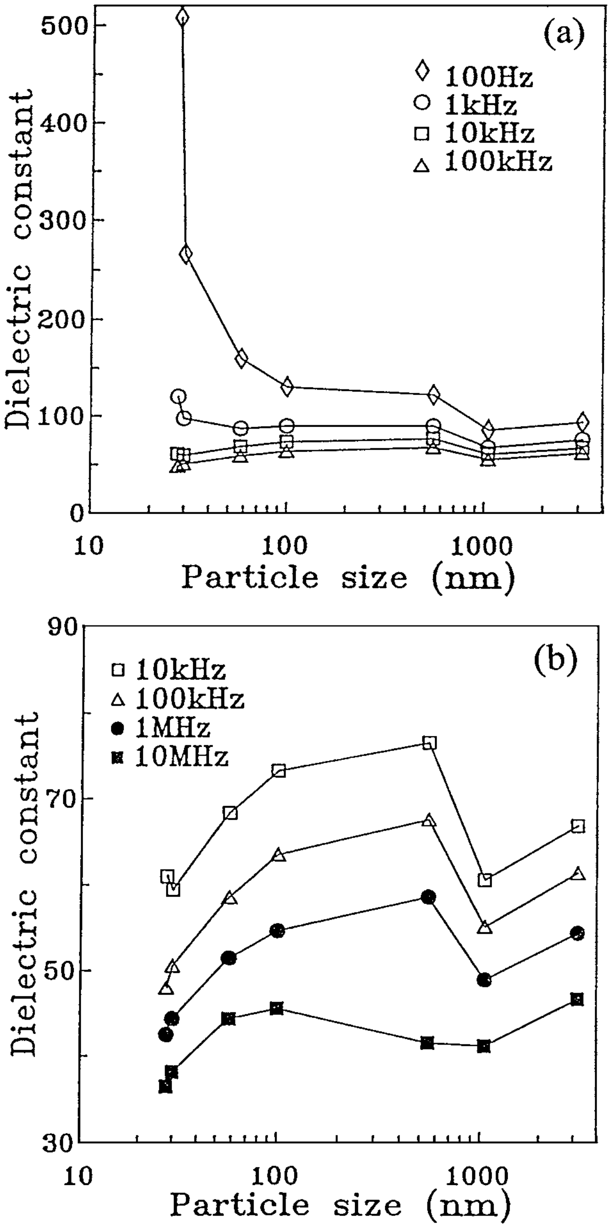

Figure 5 Variations of dielectric constant in the $BaTiO_3$/PVDF composites at varied frequency with the size of $BaTiO_3$ particles. (a) between 100 Hz and 100 kHz (b) between 10 kHz and 10 MHz.

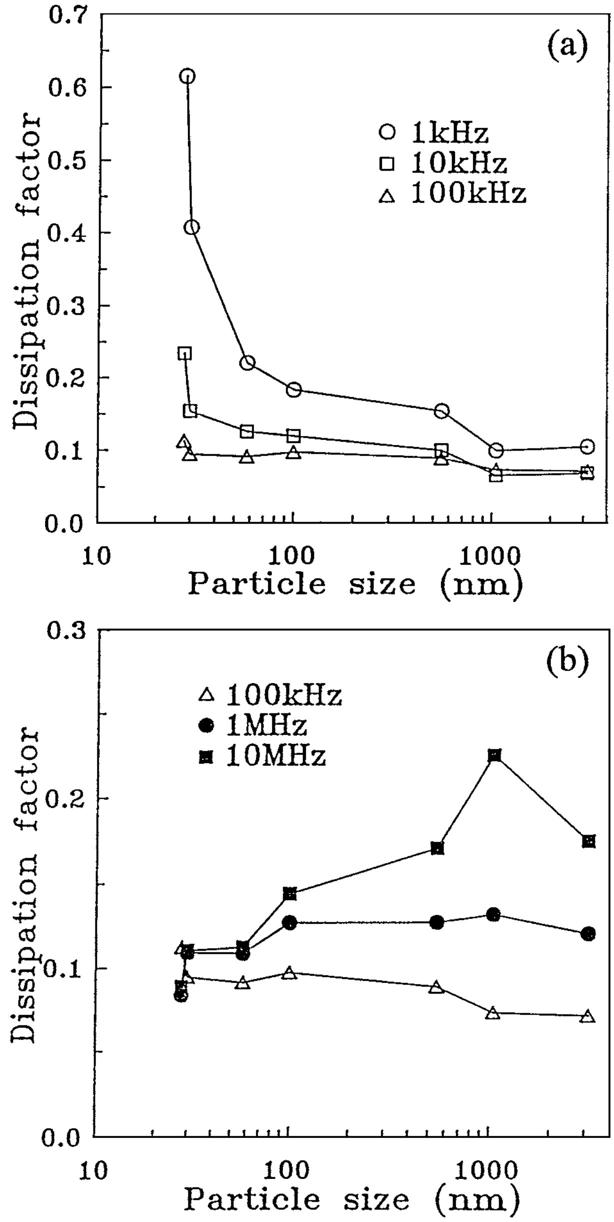

Figure 6 Variations of dissipation in the $BaTiO_3$/PVDF composites at varied frequency with the size of $BaTiO_3$ particles. (a) between 1 kHz and 100 kHz (b) between 100 kHz and 10 MHz.

during poling [25]. Table I shows the variation of the XRD intensities of (002) and (200) reflections with a poling field of 0 to 3 MV/m for composites with different $BaTiO_3$ powder sizes. The XRD intensities of (002) and (200) peaks before and after poling remain nearly unchanged for $BaTiO_3$/PVDF composites with the particle sizes below 100 nm. In composites with particle sizes larger than 100 nm, the intensity of the (200) reflection decreased and that of the (002) reflection increased after poling. With greater particle size in the tetragonal phase of $BaTiO_3$ powder, the intensity ratio increased by poling. Lee *et al.* [26] observed

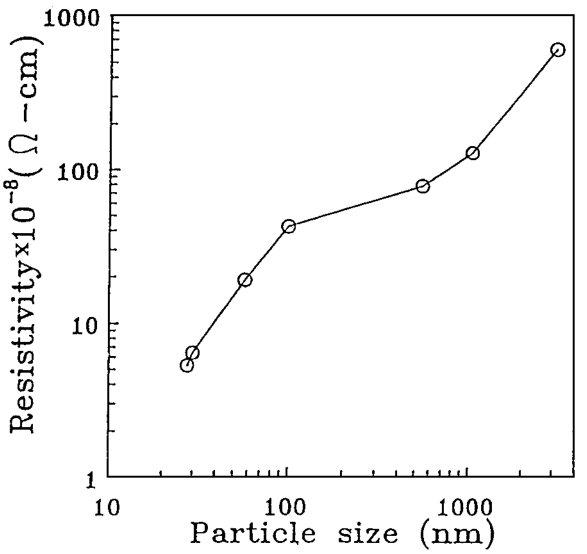

Figure 7 Variations of resistivity of composites at room temperature as a function of $BaTiO_3$ particle size.

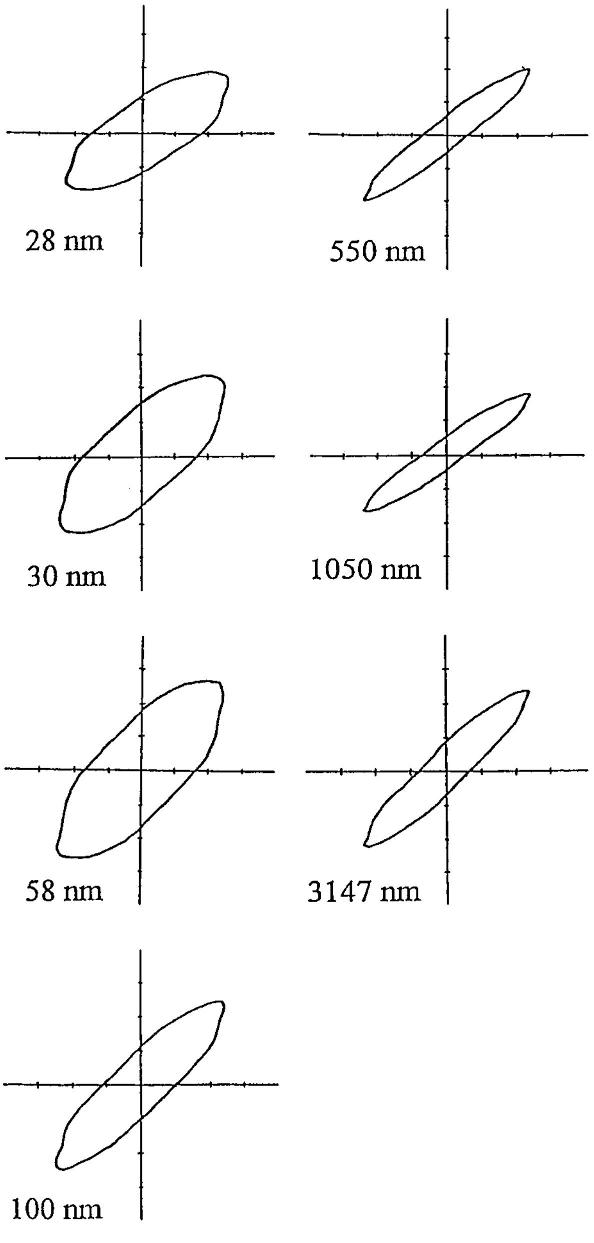

Figure 8 Hysteresis loops of $BaTiO_3$/PVDF composites with varied size of particles in $BaTiO_3$ powders. (x axis: 0.653 MV/m/div., y axis: 13.2 μC/m/div.).

that the activation energy for domain reorientation in multi-domain $PbTiO_3$ was significantly smaller than that of the activation energy for the rotation of crystallites in single domain particles during poling. Therefore, this study also indicates a probable transition from single domain to multi-domain poling behavior in $BaTiO_3$/PVDF composites with $BaTiO_3$ particle size larger than 100 nm.

3.6. Hysteresis

Fig. 8 shows hysteresis loops of the $BaTiO_3$/PVDF composites with varied size of particles in $BaTiO_3$ powders. Generally, in ferroelectric materials, the open area of the hysteresis loop diminishes with decreasing particle size. The c-$BaTiO_3$ powders calcined at lower temperature (below 900°C) were paraelectric and lacked polarization-reversal hysteresis characteristics [27]. However, in these composites, the areas of hysteresis loops decreased with increasing particle size (Fig. 8). The space charge and domain configuration of ultrafine $BaTiO_3$ powders might affect the hysteresis loop of $BaTiO_3$/PVDF composites. According to the above discussion, more numerous defects existed in $BaTiO_3$ powders with particles smaller than 58 nm (Figs 3 and 7). When the electric field is applied, the charge carriers (ionic defects) in $BaTiO_3$ powders move along the electric field, which causes power to be dissipated within the composites. The area of the hysteresis loop represents energy that is dissipated within the sample. Therefore the $BaTiO_3$/PVDF composites of particles smaller than 58 nm have broad hysteresis loops due to numerous charge carriers. When the particles of $BaTiO_3$ powders became larger than 58 nm, the hysteresis loop areas decreased, because of fewer charge carriers in $BaTiO_3$/PVDF composites. With increasing size of particles a step appears during cycling around the hysteresis loop at about 100–550 nm. It is probably resulted from the transition from single-domain to multi-domain particle because the activation energy for domain reorientation is much smaller than the activation energy for rotation of crystallites [26].

4. Conclusions

The dependence of dielectric properties of $BaTiO_3$ particles in $BaTiO_3$/PVDF composites on size is explained with space charges at the interface between $BaTiO_3$ and PVDF and domain configurations (single or multi-domain) of $BaTiO_3$ powders. For smaller $BaTiO_3$ particles, the effects of space charge on dielectric properties become dominant because of increased defects in $BaTiO_3$ powders. Therefore, the dielectric constants at frequencies <1 kHz resulting from space charge for $BaTiO_3$/PVDF composites with particles smaller than 58 nm were larger than the value observed at high frequency and the composites with small particles had broad hysteresis loops because of more numerous charge carriers. For particles of $BaTiO_3$ powders larger than 58 nm, the hysteresis loop areas decreased largely due to fewer charge carriers in $BaTiO_3$/PVDF composites. With increasing particle size a step that appears during poling and cycling around the hysteresis loop at about 100–650 nm may be due to the transition from single domain to multi-domain particles.

References

1. T. FURUKAWA, K. FUJINO and E. FUKADA, *Jpn. J. Appl. Phys.* **15** (1976) 2119.
2. R. E. NEWNHAM, *Ferroelectrics* **68** (1986) 1.
3. R. Y. TING, *ibid.* **67** (1986) 143.
4. C. MURALIDHAR and P. K. C. PILLAI, *J. Mater. Sci.* **23** (1988) 410.
5. G. ARLT, D. HENNING and G. DE. With, *J. Appl. Phys.* **58** (1985) 1619.
6. G. ARLT, *J. Mater. Sci.* **25** (1990) 2655.
7. W. R. BUESSEM, L. E. CROSS and A. K. GOSWAMI, *J. Amer. Ceram. Soc.* **49** (1966) 36.
8. T. KANATA, T. YOSHIKAWA and K. KUBOTA, *Solid State Communication* **62** (1987) 765.
9. J. M. HERBERT, in “Ceramic Dielectrics and Capacitors” (Gordon and Beach Science, New York, 1985) p. 136.
10. G. H. JONKER, *J. Amer. Ceram. Soc.* **55** (1972) 57.
11. H. G. LEE and H. G. KIM, *J. Appl. Phys.* **67** (1990) 2024.
12. A. K. GOSWAMI, *ibid.* **40** (1969) 619.
13. R. E. NEWNHAM and S. E. TROLIER-MCKINSTRY, *Ceramic Transaction* **8** (1990) 235.
14. H. I. HSIANG and F. S. YEN, *Jpn. J. Appl. Phys.* **33** (1994) 3991.
15. R. SEKAR, A. K. TRIPATHI and P. K. C. PILLAI, *Mater. Sci. Eng.* **B5** (1989) 33.
16. C. MURALIDHAR and P. K. C. PILLAI, *J. Mater. Sci. Lett.* **6** (1987) 1243.
17. *Idem.*, *Mat. Res. Bull.* **22** (1987) 1703.
18. D. CULLITY, “Elements of X-Ray Diffraction” (Addison-Wesley Press, Menlo Park, 1978) p. 102.
19. J. ALLEN, “Particle Size Measurement” (Chapman and Hall, New York, 1981) p. 27.
20. H. P. KLUG and L. E. ALEXANDER, “X-Ray Diffraction Procedures for Polycrystalline and Amorphous Materials” (Carnegie-Mellon University Press, New York, 1973) p. 618.
21. G. ARLT, *J. Mater. Sci.* **25** (1990) 2655.
22. F. S. YEN, C. T. CHANG and Y. H. CHANG, *J. Amer. Ceram. Soc.* **73** (1990) 34
23. C. MURALIDHAR and P. K. C. PILLAI, *J. Mater. Sci.* **23** (1998) 1071.
24. G. ARLT, *Ferroelectrics* **104** (1990) 217.
25. M. H. LEE, A. HALLIYAL and R. E. NEWNHAM, *J. Amer. Ceram Soc.* **72** (1989) 986.
26. *Idem.*, *Ferroelectrics* **87** (1988) 71.
27. M. H. FREY and D. A. PAYNE, *Appl. Phys. Lett.* **63** (1993) 2753.

Received 23 April 1999
and accepted 23 January 2001